Life Sciences 239 (2019) 116881

Contents lists available at ScienceDirect

Life Sciences

journal homepage: www.elsevier.com/locate/lifescie

Salvianolic acid B exerts anti-liver fibrosis effects *via* inhibition of MAPK-mediated phospho-Smad2/3 at linker regions *in vivo* and *in vitro*

Chao Wu[a,b], Weiyang Chen[a], Hanyan Ding[a], Dong Li[a], Guanghua Wen[a], Chong Zhang[a], Wanpeng Lu[a], Ming Chen[a], Yan Yang[a,*]

[a] Department of Pharmacology, Anhui Medical University, Key Laboratory of Anti-inflammatory and Immunopharmacology, Ministry of Education, 81 Meishan Road, Hefei, 230032, China

[b] Department of Pharmacy, The First Affiliated Hospital of Anhui University of Chinese Medicine, 117 Meishan Road, Hefei, 230031, China

ARTICLE INFO

Keywords:
Salvianolic acid B
Liver fibrosis
Transforming growth factor-beta
Mitogen-activated protein kinase
Smad2/3 phosphoisoforms

ABSTRACT

Aim: To investigate anti-liver fibrosis effects of Salvianolic acid B (Sal B) from *Salvia miltiorrhiza* Bunge involved mitogen-activated protein kinase (MAPK)-mediated transforming growth factor-beta (TGF-β) signaling.

Main methods: Diethylnitrosamine (DEN)-induced liver fibrosis in mice and TGF-β_1-activated hepatic stellate cells (HSCs) were established and treated with dosage/concentration-graded Sal B and/or MAPK activator (Vacquinol-1: MKK4-specific activator)/inhibitors (PD98059: ERK-specific inhibitor; SP600125: JNK-specific inhibitor; SB203580: p38-specific inhibitor). Histopathological characteristics and cell migration were assessed, α-SMA, Collagen I and members of TGF-β/MAPK/Smad signal transduction pathway were measured.

Key findings: Results *in vivo* showed that Sal B alleviated DEN-caused liver fibrosis embodied in ameliorative histopathological characteristics and decreased protein levels of hepatic fibrosis related markers (α-SMA, Collagen I, TGF-β_1), its molecular mechanisms of action were correlative with inhibited activation of MAPK and phosphorylation of Smad2/3 at linker regions (P-Smad2/3L) and Smad2 at C-terminal (P-Smad2C) while increased phosphorylation of Smad3 at C-terminal (P-Smad3C). Results *in vitro* showed that Sal B restrained TGF-β_1-induced HSCs activation, Collagen I production and cell migration; Sal B inhibited activation of MAPK and markedly decreased protein levels of P-Smad2/3L and P-Smad2C while slightly increased P-Smad3C in TGF-β_1-stimulated HSCs, the expression of PAI-1 was inhibited by Sal B; activating MAPK receded inhibitory effects of Sal B on α-SMA, Collagen I, P-Smad2L and P-Smad3L expression while inhibited activation of MAPK reinforced those.

Significance: Sal B attenuates liver fibrosis *via* mediation of TGF-β/Smad and MAPK pathways, especially inhibition of MAPK-mediated P-Smad2/3L signaling, which maybe provides theoretical foundation of Sal B for treating clinically liver fibrosis.

1. Introduction

Clinically, liver fibrosis is pathologically pervasive in the progress of various chronic liver diseases, such as viral hepatitis, alcoholic liver disease, non-alcoholic fatty liver disease (NAFLD), autoimmune liver disease (ALDS), drug-induced liver injury, etc; if controlled ineffectively, liver fibrosis can advance into cirrhosis and subsequently soaring risk of hepatocarcinogenesis [1]. Actually, liver fibrosis is a common outcome from abnormal wound-healing to chronic liver injury caused by multifarious etiologies, which is hopefully reversed and then obtained cure [2]. Under chronic liver injury, hepatic stellate cells (HSCs) originally remaining quiescent in healthy liver are persistently activated by endogenous pro-fibrogenic cytokines and/or pro-inflammatory factors originated from injured hepatocytes, Kupffer cells and/or inflammatory cells, activated HSCs produce excessive synthesis while inhibited degradation of collagen contributing to accumulation of extracellular matrix (ECM), which is deemed as the central pathophysiologic mechanism leading to liver fibrosis [3]. Transforming growth

Abbreviations: α-SMA, alpha smooth muscle actin; Collagen I, type I collagen; TGF-β_1, transforming growth factor-beta 1; MAPK, mitogen-activated protein kinase; ERK, extracellular signal-regulated kinase; JNK, c-Jun N-terminal kinase; MKK4, mitogen-activated protein kinase kinase 4; P-Smad2C, $Ser^{465/467}$ C-terminally phosphorylated Smad2; P-Smad2L, $Ser^{250/255}$ linker phosphorylated Smad2; P-Smad3C, $Ser^{423/425}$ C-terminally phosphorylated Smad3; P-Smad3L, $Ser^{208/213}$ linker phosphorylated Smad3; PAI-1, plasminogen activator inhibitor 1

* Corresponding author.
E-mail address: yangyan@ahmu.edu.cn (Y. Yang).

https://doi.org/10.1016/j.lfs.2019.116881
Received 5 July 2019; Received in revised form 13 September 2019; Accepted 16 September 2019
Available online 31 October 2019
0024-3205/

factor beta type I (TGF-β_1), a ubiquitous cytokine participating in mostly physiological and pathological processes such as growing development and disease pathogenesis, is widely accepted as one of the strongest pro-hepatofibrogenic cytokines [4,5].

TGF-β_1 generates bio-effects *via* TGF-β signaling, which is differentially regulated by dynamism of phosphorylated Smad2/3 mediators [6]. Concretely, TGF-β_1 combines with TGF-β receptor type II (TβRII), then recruits and *trans*-phosphorylates TGF-β receptor type I (TβRI), subsequently phosphorylated TβRI directly activates Smad2/3 at C-terminal to form activated Smad2C and Smad3C (P-Smad2C and P-Smad3C); otherwise, TGF-β signaling employs intracellular activated mitogen-activated protein kinases (MAPKs) including extracellular signal-regulated kinase (ERK), c-Jun N-terminal kinase (JNK) and p38 to phosphorylate Smad2/3 at linker regions resulting in activated Smad2L and Smad3L (P-Smad2L and P-Smad3L) [7]. Certainly, P-Smad2L depending on P-Smad2C and P-Smad3L respectively transmit pro-metastatic and/or pro-fibrogenic signaling and mitogenic signaling to contribute to fibrogenesis and malignant progression *via* mediating the expression of downstream target genes such as plasminogen activator inhibitor 1 (PAI-1), crucial mediator involved in ECM deposition and cell migration/invasion, which is a functional protein closely related to liver fibrosis [8,9]; P-Smad3C transmits cytostatic signaling, which plays a protecting against liver fibrosis role *via* promoting the expression of p21, a critical target gene of downstream associated with mediating cell cycle [9,10]. In view of crucial and distinctive impacts of Smad2/3 phosphoisoforms involved in the development of liver fibrosis, targeting Smad2/3 phosphoisoforms especially inhibiting MAPK-mediated phospho-Smad2/3 at linker regions to correct aberrant TGF-β signaling in liver fibrosis is a novel and efficient tactic for developing therapeutic drugs against liver fibrosis.

Salvianolic acid B (Sal B) is deemed as the major active component of water-soluble extracts phenolic acids (Accounting approximately for 70% of phenolic acids) derived from *Salvia miltiorrhiza* Bunge [11], which is a traditional Chinese herb commonly used for treating cardiovascular and hepatic diseases [12,13]. Sal B has been reported to ameliorate both patients with liver fibrosis chronically infected hepatitis B virus (HBV) and rats with liver fibrosis induced by tetrachloromethane (CCl_4) or dimethylnitrosamine (DMN) *in vivo* as well as inhibit cell proliferation and collagen production of rat primary HSCs, induce apoptosis of liver fibrotic cells from mice and rat-HSCs involved in mediating TGF-β signaling [14–18], which suggest Sal B is a potential candidate for liver fibrosis treatment, however, the evidences are insufficient about pinpoint mechanisms of Sal B on liver fibrosis. The study was aimed at investigating the effect of Sal B on liver fibrosis related to Smad2/3 phosphoisoform signaling, particularly the MAPK-mediated Smad2/3 phosphorylated at linker regions in models *in vivo* [Diethylnitrosamine (DEN)-induced liver fibrosis] and *in vitro* (TGF-β_1-stimulated rat HSC-T6 and human LX-2 cells) of liver fibrosis.

2. Materials and methods

2.1. Chemicals and antibodies

Salvianolic acid B (Sal B), a novel water-soluble monomer rooted from *Salvia miltiorrhiza* Bunge, was purchased from Chengdu PUSH Biotechnology Co. LTD (Chengdu, China). The purity of Sal B (CAS No: 121521-90-2) was 99.45% (Lot No: PS14120501) used *in vitro* experiments and 97.63% (Lot No: PS12091001) *in vivo* experiment, molecular weight 718.61, molecular formula $C_{36}H_{30}O_{16}$, and chemical structure shown in Fig. 1D. Diethylnitrosamine (DEN, Cat # 73861, CAS No: 55-18-5; 0.95 g/ml, purity ≥ 99.0%) was obtained from Sigma-Aldrich (St Louis, USA). Masson's trichrome staining kit (Cat # MST-8003) was purchased from Maixin-Bio (Fuzhou, China), Immunohistochemical staining kit (Cat # PV-6000) from OriGene Technologies, Inc. (Rockville, USA), cell lysis buffer for Western and IP (Cat #P0013) from Beyotime (Shanghai, China). Recombinant human TGF-β_1 (Cat # 100-21C) was obtained from PeproTech (Rocky Hill, USA), MKK4-specific activator (Vacquinol-1, Cat #S7544, CAS No: 5428-80-8, purity > 99.0%) from Selleck (Houston, USA); ERK-specific inhibitor (PD98059, Cat # 513000), JNK-specific inhibitor (SP600125, Cat # 420128) and p38 -specific inhibitor (SB203580, Cat # 559389) were obtained from Calbiochem (San Diego, USA); used primary antibodies (Abs) included mouse monoclonal anti-α-SMA Ab (Cat # bsm-33188 M), rabbit polyclonal anti-Collagen I Ab (Cat # bs-10423R) and anti-GAPDH Ab (Cat # bs-2188R) (Bioss; Beijing, China), rabbit polyclonal anti-TGF-β_1 Ab (Cat # sc-146) (Santa Cruz Biotechnology, Inc.; Santa Cruz, USA), rabbit polyclonal anti-P-ERK1/2 (Thr^{202}/Thr^{204}) Ab (Cat # 9101), anti-ERK1/2 Ab (Cat # 9102), anti-P-JNK1/2 (Thr^{183}/Tyr^{185}) Ab (Cat # 4668), anti-JNK1/2 Ab (Cat # 9252), anti-P-p38 (Thr^{180}/Thr^{182}) Ab (Cat # 9211), anti-p38 Ab (Cat # 9212), anti-P-Smad2C ($Ser^{465/467}$) Ab (Cat # 3101), anti-P-Smad3C ($Ser^{423/425}$) Ab (Cat # 9520) (Cell Signaling Technology; Danvers, USA), rabbit anti-Smad2 Ab (Cat # ab40855) (Abcam; Cambridge, UK), rabbit anti-Smad3 Ab (Cat # 25494-1-AP) (PeproTech; Rocky Hill, USA), rabbit polyclonal anti-P-Smad2L ($Ser^{250/255}$) Ab (Cat # 28025) and anti-P-Smad3L ($Ser^{208/213}$) Ab (Cat # 38274) (Gifts from Dr. K. Matsuzaki, Department of Gastroenterology and Hepatology, Kansai Medical University, Osaka, Japan), rabbit polyclonal anti-PAI-1 Ab (Cat # PA5-27216) (Thermo Fisher Scientific; Waltham, USA), mouse monoclonal anti-GAPDH Ab (Cat # TA-08) (OriGene Technologies, Inc.; Rockville, USA); corresponding secondary antibodies included peroxidase-conjugated goat anti-mouse immunoglobulin G (IgG; H + L) (Cat # ZB-2305), peroxidase-conjugated goat anti-rabbit lgG (Cat # ZB-2301) (OriGene Technologies, Inc.; Rockville, USA); SuperSignal™ West Femto Substrate Trial Kit (Cat # 2161462) was obtained from Thermo Fisher Scientific (Waltham, USA).

2.2. DEN-induced liver fibrosis in mice and Sal B treatment

Matured male Kunming mice (SPF grade) weighing 20 ± 2 g with an age of 6 weeks were obtained from Laboratory Animal Center of Anhui Medical University, where was elected as the place of the animal experiment performed. The mice were housed in ventilated plastic cages with a controlled raising environment (20–22 °C, 40–70% relative humidity, 12-h light-dark cycle, standard mouse feedstuff and water *ad libitum*). Animal use and care in the study were followed the Regulations of Experimental Animal Administration set by State Scientific and Technological Commission of People's Republic of China, and experimental protocols were approved by the Experimental Animal Ethics Committee of Anhui Medical University.

After acclimatization for 1 week, these mice were randomly allocated into following four groups (N = 10): control group, DEN group, DEN + Sal B (15 mg/kg) group, DEN + Sal B (30 mg/kg) group. Models of DEN-induced liver fibrosis in mice excluded those in control group were established by injecting intraperitoneally with 1.0% DEN (10 ml/kg) diluted into sterile normal saline (NS), once a week for 12 weeks; Sal B with corresponding doses dissolved in sterile NS (Prepared when using) were administrated by gavage in mice of corresponding groups respectively (Operating in dark place), once a day for 12 weeks; meanwhile, mice in control group were administrated with NS (Solvent) only. Animal models established/Sal B-administration and subsequent analyses were carried out in a blinded fashion (Experimental operators without above knowledge) for above all groups. These mice were sacrificed using cervical dislocation under sodium pentobarbital (I.P, 80 mg/kg) anaesthesia and livers were harvested. One liver lobule from each liver was fixed in 10% formalin, then dehydrated in graded alcohol series, embedded in paraffin and cut into 4 mm sections, which were used for histopathological examination and Immunohistochemical staining analysis. The others from each liver were stored at −80 °C for Western blot analysis.

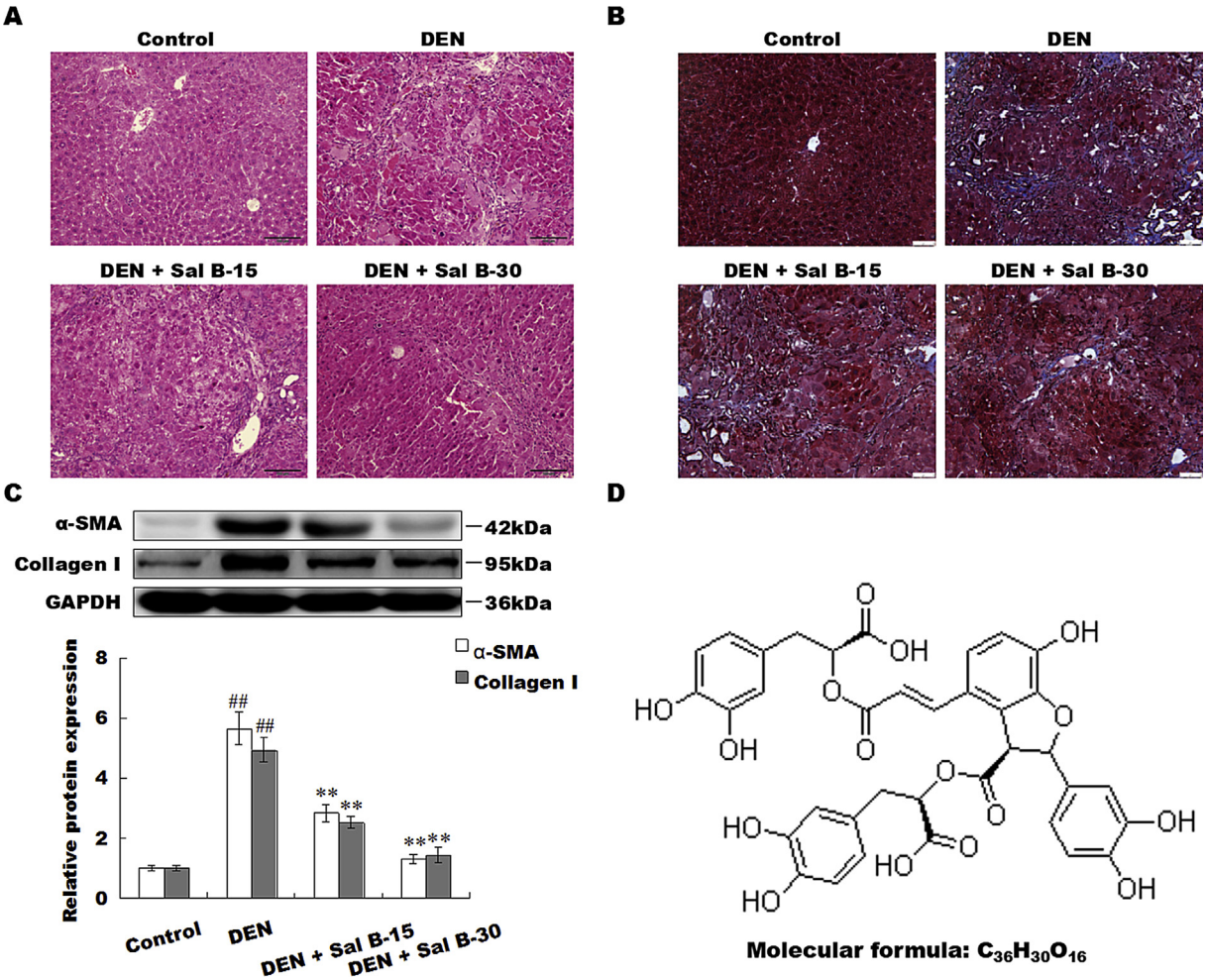

Fig. 1. Sal B ameliorated DEN-induced liver fibrosis reflected in ameliorative histopathological characteristics and hepatic-fibrosis markers in mice. (A) Histopathological characteristics of mouse liver sections were assessed with hematoxylin and eosin (H&E) staining and representative image in each group was presented (Magnification × 200). (B) Collagen fibers (Blue color) in mouse liver sections were specifically visualized by Masson's trichrome staining and representative image in each group was presented (Magnification × 200). (C) Hepatic-fibrosis markers including α-SMA and Collagen I from mouse liver tissues were measured by Western blot and representative images in each group were presented. Semiquantitative analyses of α-SMA and Collagen I protein levels were respectively conducted, GAPDH was deemed as the loading control and the ratio of α-SMA or Collagen I protein to GAPDH in control group was assigned a value of 1. Data were expressed as mean ± SD, n = 3. $^{\#\#}P < 0.01$ versus Control group; $^{**}P < 0.01$ versus DEN group. (D) The chemical structure of Sal B. (For interpretation of the references to color in this figure legend, the reader is referred to the Web version of this article.)

2.3. Cell cultivation and treatment

Two immortalized hepatic stellate cell lines, HSC-T6 originated from rat and LX-2 from human were purchased from the Chinese Academy of Science Cell Bank (Shanghai, China). The two cells were maintained with Dulbecco's modified Eagle's medium (DMEM; Hyclone; Logan, USA) supplemented with 10% fetal bovine serum (FBS; Sijiqing, Zhejiang Tianhang Biological Technology Co., LTD; Huzhou, China) in a humidified incubator with an atmosphere of 5% CO_2 at 37 °C. These cells at logarithmic growth were collected, counted and seeded at a density of 1×10^6 cells/25 cm^2 culture flask cultured in DMEM supplemented with 10% FBS. When these cells reached 80–90% confluency, the medium was replaced using serum-free medium with or without Sal B (25 μM, 50 μM, 100 μM) for 24 h and TGF-β_1 (9 pM) was added for 1 h, total proteins were extracted for followed Western blot analysis. Additionally, HSCs named HSC-T6 cells were cultured with or without Sal B (50 μM) for 24 h and MKK4-specific activator (Vacquinol-1; 15 μM), ERK-specific inhibitor (PD98059; 10 μM), JNK-specific inhibitor (SP600125; 10 μM) and p38-specific inhibitor (SB203580; 10 μM) for 5 h, TGF-β_1 (9 pM) for 1 h, total proteins were extracted.

2.4. Cell migration assay

Cell migration was detected using Scratch test as described previously [19]. The two cells (HSC-T6 and LX-2) at logarithmic phase were collected, counted and seeded in 6-well plates at a density of 5×10^5 cells/well and cultured in DMEM supplemented with 10% FBS, respectively. When these cells reached 90% confluency, complete medium was replaced with free-serum medium for overnight to synchronize these cells, then a sterile 200 μl pipette tip was used to scratch three horizontal and three vertical streaks on the well inner surface and these cells were incubated with or without Sal B (25 μM, 50 μM, 100 μM) and TGF-β_1 (60 pM) for 24 h. Image acquisition with scratch area was performed at 0, 12, 24 h window respectively using a light microscope (Olympus, Tokyo, Japan), the width of scratch area was measured, Healing rate of scratch (%) was calculated according to the following formula: Healing rate of scratch (%) = (the width of scratch area at 0 h - the width of scratch area at 12/24 h) ÷ the width of scratch area at 0 h × 100%.

2.5. Histopathological examination

Histopathological characteristics of livers were examined using hematoxylin and eosin (H&E) staining performed as standard procedure. Briefly, paraffin sections were deparaffinized in xylene and graded alcohols orderly, rehydrated in distilled water, stained in hematoxylin dye and blued in running water, then stained in eosin and finally mounted using neutral balsam. Collagen fibers were visualized with the blue color using Masson's trichrome staining kit performed as the manufacturer's instruction. To summarize, paraffin sections were routinely deparaffinized and rehydrated, then stained in Masson's compound staining fluid constituted of Biebrich's scarlet-acid fuchsin and Weigert's iron hematoxylin, washed in distilled water, stained in phosphomolybdic acid and dried, then stained in aniline blue solution and rinsed in 1% acetic acid solution, whereafter dehydrated in graded alcohols and xylene orderly, finally mounted using neutral balsam. These stained sections were imaged using a Intelligent Positive Fluorescence Microscope (Leica Microsystems, Mannheim, Germany). Histological scores for fibrosis severity from all samples in each groups were performed based on the criteria reported previously [20,21], which was presented as follow: score 0, normal; score 1, fibrosis present (Collagen fibers extended from the portal triad or central vein to peripheral regions); score 2, mild fibrosis (Collagen fibers presented with extension without compartment formation); score 3, moderate fibrosis (Collagen fibers presented with some pseudolobe formation); score 4, severe fibrosis (Severe collagen fibers presented with thickening of the partial compartments and frequent pseudo lobe formation).

2.6. Immunohistochemical staining analysis

The expression and distribution of P-Smad2C, P-Smad2L, P-Smad3C, P-Smad3L in liver tissues were detected by Immunohistochemical staining using Immunohistochemical staining kit performed as the manufacturer's instruction. Simply put, paraffin sections were routinely deparaffinized and rehydrated, then antigen retrieval was done by heating these sections to 121 °C in 0.01 mol/L sodium citrate buffer (pH 6.0) (BOSTER; Wuhan, China) for 10 min, after cooling down and washing with phosphate buffer solution (PBS) for 3 times at 3 min each time (The same below), these sections were incubated in 3% H_2O_2 for 10 min at 37 °C to block endogenous peroxidase and then washed with PBS. The non-specific antibody binding sites were blocked with normal goat serum working solution for 15 min at 37 °C. The sections were incubated with rabbit polyclonal anti-P-Smad2C (1:100), rabbit polyclonal anti-P-Smad3C (1:100), rabbit polyclonal anti-P-Smad2L (1:50) and rabbit polyclonal anti-P-Smad3L (1:50) Abs overnight at 4 °C respectively. Next day, The sections were rewarmed at 37 °C for 20 min and washed with PBS, then incubated with peroxidase-labeled polymer conjugated goat anti-rabbit lgG for 20 min at 37 °C and washed with PBS. These sections were developed with 3, 3′-diaminobenzidine (DAB) (ZLI-9018; OriGene Technologies, Inc.; Rockville, USA) and counterstained with hematoxylin, finally, mounted with neutral balsam. The stained sections were imaged using an Intelligent Positive Fluorescence Microscope (Leica Microsystems; Mannheim, Germany), results were evaluated by ImageJ2x software (NIH; Bethesda, USA), assigning score based on the percentage of positive-stained cells.

2.7. Western blot analysis

Protein levels of hepatic fibrosis markers α-SMA and Collagen I, members of TGF-β/MAPK/Smad signaling transduction pathway in both liver tissues and HSCs were measured using Western blot analysis performed as described previously [22]. Total proteins from liver tissues and/or HSCs were extracted using a cell lysis buffer (P0013; Beyotime; Shanghai, China) according to the manufacturer's instruction, protein concentrations in these samples were measured with BCA protein assay kit (P0012S; Beyotime; Shanghai, China). Detected proteins were segregated by sodium dodecyl sulfate/polyacrylamide gel electrophoresis (SDS/PAGE), and then transferred onto polyvinylidence difluoride (PVDF) membranes (Millipore; Bedford, USA) by wet transfer method. These PVDF membranes were immersed in 5% skim milk powder for 2 h at room temperature to block non-specific antibody binding, then incubated with primary antibodies including mouse anti-α-SMA (1:1000), rabbit anti-Collagen I (1:500), rabbit anti-TGF-β_1 (1:1000), rabbit anti-P-ERK1/2 (1:1000), rabbit anti-ERK1/2 (1:1000), rabbit anti-P-JNK1/2 (1:1000), rabbit anti-JNK1/2 (1:1000), rabbit anti-P-p38 (1:1000), rabbit anti-p38 (1:1000), rabbit anti-P-Smad2C (1:1000), rabbit anti-P-Smad2L (1:500), rabbit anti-Smad2 (1:5000), rabbit anti-P-Smad3C (1:1000), rabbit anti-P-Smad3L (1:500), rabbit anti-Smad3 (1:2000), rabbit anti-PAI-1 (1:2000), mouse anti-GAPDH (1:10000) and rabbit anti-GAPDH (1:5000) Abs overnight at 4 °C respectively. After washing with Tris-buffered saline solution/0.1 Tween 20 (TBST) for 3 times (10 min each time), these PVDF membranes were incubated with appropriate secondary antibodies with peroxidase-conjugated including peroxidase-conjugated goat anti-rabbit lgG (1:10000) and peroxidase-conjugated goat anti-mouse lgG (1:10000) for 2 h (Room temperature), then washed with TBST (The same above), finally, developed using SuperSignal™ West Femto Substrate Trial Kit under ChemiDoc™MP Imaging System (Bio-Rad; Hercules, USA). These results were analyzed by ImageJ2x software.

2.8. Statistic analysis

Quantitative data were presented as mean ± standard deviation (SD). Statistic analysis was performed using SPSS 16.0 software for Windows (SPSS, Inc.; Chicago, USA). Difference of fibrosis grade between groups was performed by the Mann-Whitney test, differences of remaining data among groups were analyzed using one-way analysis of variance (ANOVA) with Least Significant Difference (LSD) as a post-hoc test, $P < 0.05$ was regarded as statistically significant.

3. Results

3.1. Sal B ameliorated DEN-induced liver fibrosis reflected in ameliorative histopathological characteristics and hepatic-fibrosis markers in mice

Anti-liver fibrosis effects of Sal B *in vivo* were assessed by histopathological examination and hepatic-fibrosis markers. H&E staining showed that normal liver histological structures from normal mice in control group were observed, pathological changes with hepatic lobules segmented by collagen bundles and tissue spaces padded inflammatory cells in liver sections from mice in DEN group were presented, while Sal B (15 mg/kg, 30 mg/kg) co-administration markedly ameliorated above lesions resulted from DEN (Fig. 1A). Masson's trichrome staining was performed to specifically visualize collagen fibers, which revealed that extensive collagen fibers were observed in DEN group, while Sal B dose-dependently decreased the deposition of collagen fibers (Fig. 1B). Staging score of liver fibrosis showed that a significantly elevated score was observed in DEN group compared to that in control group, while dose-dependently lowered scores were presented in the above two doses of Sal B co-administration groups compared to that of DEN group (Table 1). α-SMA, a biomarker of HSC activated, and Collagen I, the dominant component of ECM, above two proteins are common hepatic-fibrosis markers to reflect the degree of fibrosis. Our results showed that Sal B dose-dependently decreased the protein levels of α-SMA and Collagen I compared to those of DEN group (Fig. 1C). These results demonstrate that Sal B can observably ameliorate DEN-induced liver fibrosis in mice.

Table 1
Liver fibrosis grade in each group of mice.

Group	N	Staging score of liver fibrosis					
		0	1	2	3	4	Mean ± SD
Control	10	10	0	0	0	0	0.00 ± 0.000
DEN	9	0	0	0	3	6	3.67 ± 0.500##
DEN + Sal B-15	9	0	0	3	5	1	2.78 ± 0.667*
DEN + Sal B-30	10	0	4	4	2	0	1.80 ± 0.789**

Significance was determined by the Mann–Whitney test; death occurred in DEN group (1/10) and DEN + Sal B (15 mg/kg) group (1/10) before mice harvested. ##$P < 0.01$ versus Control group; *$P < 0.05$,**$P < 0.01$ versus DEN group.

3.2. Sal B repressed hepatic-fibrosis markers expression and cell migration in TGF-β_1-stimulated HSCs

To further evaluate Sal B's anti-liver fibrosis effects *in vitro*, hepatic-fibrosis markers (α-SMA, Collagen I) and cell migration ability were measured using Western blot and Scratch test in HSCs (Including two cell lines: rat HSC-T6 and human LX-2) stimulated by TGF-β_1 respectively. Our results showed that Sal B (25 μM, 50 μM, 100 μM) inhibited activation of both HSC-T6 and LX-2 cells induced by TGF-β_1 reflected in decreased protein expression of α-SMA compared to that of TGF-β_1 (9 pM) stimulated group, and inhibited Collagen I production (Fig. 2A and B). Cell migration of activated HSCs, a dominant factor leading to the progression of liver fibrosis, was observed obvious enhancement in both HSC-T6 and LX-2 cells induced by TGF-β_1 (60 pM) for 12 h and 24 h, however simultaneously, Sal B (25 μM, 50 μM, 100 μM) co-administration significantly inhibited cell migration of above two HSCs in a dose-dependent manner compared to that of TGF-β_1 stimulated group (Fig. 2C and D). These results demonstrate that Sal B can inhibit TGF-β_1-induced activation of HSCs accompanied by attenuated Collagen I production and cell migration.

3.3. Sal B inhibited the activation of MAPK pathways and modulated the phosphorylation of Smad2/3 in mice with DEN-induced liver fibrosis

Considering that TGF-β signaling, particularly transmits *via* activating MAPKs and subsequently phosphorylating Smad2/3 at linker regions, plays a crucial role in liver fibrogenesis-progress, we investigated the molecular mechanism of Sal B protecting against liver fibrosis involved in TGF-β_1/MAPK/Smad2/3 signal transduction axis *in vivo*. TGF-β_1 and activated MAPKs including P-ERK1/2, P-JNK1/2 and P-p38 in frozen liver tissues from mice of each group were measured using Western blot. Our results showed that dramatically increased protein expressions of TGF-β_1, P-ERK1/2, P-JNK1/2 and P-p38 were observed in DEN group, while Sal B co-administration decreased above protein levels in a dose-dependent manner (Fig. 3A and B). Phosphorylated Smad2/3 at C-terminal included P-Smad2C/P-Smad3C and linker regions included P-Smad2L/P-Smad3L in liver tissues were detected using Immunohistochemical staining. Our results showed that markedly increased positive cells with P-Smad2C, P-Smad2L and P-Smad3L were observed in liver sections, especially the liver areas with fibrotic lesions from mice of DEN group, while in combination with Sal B treatment dose-dependently decreased the amounts of P-Smad2C-, P-Smad2L-, P-Smad3L-positive cells; moreover, Sal B observably increased P-Smad3C-positive cells in relatively normal liver areas only (Fig. 3C). Protein levels of P-Smad2C and P-Smad2L in frozen liver tissues from each group were measured using Western blot, which showed remarkable increase of P-Sma2C and P-Smad2L protein expression in DEN group, while Sal B co-administration resulted in dose-dependent decrease of above two proteins compared to those of DEN-group (Fig. 3D). These results indicate that Sal B exerts anti-liver fibrosis effects intimately involved in mediated TGF-β_1/MAPK/Smad2/3 signal transduction.

3.4. Sal B modulated MAPK pathways activation and Smad2/3 phosphorylation in TGF-β_1-stimulated HSCs

To investigate the effects of Sal B on intracellular employees principally including MAP kinases (ERK1/2, JNK1/2 and p38) and Smad family (Smad2/3) of TGF-β signaling, HSCs (HSC-T6 and LX-2 cells) were pretreated with Sal B (25 μM, 50 μM, 100 μM) for 24 h and followed TGF-β_1 (9 pM) added to activate TGF-β signaling for 1 h, the activation of MAPKs and Smad2/3 phosphoisoforms (C-terminal and linker region) measured using Western blot. Our results showed that increased P-ERK1/2, P-JNK1/2, P-p38, P-Smad2C, P-Smad2L, P-Smad3C and P-Smad3L were observed in both HSC-T6 and LX-2 cells induced by TGF-β_1, while Sal B pretreatment resulted in notably decreased above protein expressions excluded slightly increased P-Smad3C in a concentration-dependent manner (Fig. 4). These results indicate that Sal B modulates TGF-β signaling *via* inhibiting the activation of MAPK pathways and mediating Smad2/3 phosphorylation at C-terminal and linker regions in TGF-β_1-stimulated HSCs.

3.5. Sal B down-regulated PAI-1 protein expression in TGF-β_1-stimulated HSCs

The expression of PAI-1, deemed as direct target gene of TGF-β signaling and closely related to fibrogenesis and progression, was measured in this study. Our results showed that TGF-β_1 increased the expression of PAI-1 protein in both HSC-T6 and LX-2 cells, while Sal B concentration-dependently decreased PAI-1 protein level in above two cell lines of HSC (Fig. 5). These results indicate that Sal B down-regulates PAI-1 expression in TGF-β_1-stimulated HSCs.

3.6. MAPK activator receded inhibitory effects of Sal B on HSCs activation and Collagen I production involved in enhancement of Smad2/3 linker regions phosphorylation

We further verified Sal B's anti-liver fibrosis effects involved in mediating Smad2/3 phosphorylation at linker regions in a MAPK-dependent manner. A MKK4-specific activator named Vacquinol-1 was used to activate MAPK pathways, whereafter we compared inhibitory effects of Sal B (50 μM) on HSCs activation and Collagen I production involved in Smad2/3 linker regions phosphorylation. Our results showed that up-regulated protein levels of P-MAPKs (Including P-JNK1/2 and P-p38 rather than P-ERK1/2) in Vacquinol-1 treatment-group were observed, while Sal B treatment lowered above protein levels and these protein levels were higher than those in Sal B alone treatment group; simultaneously, homodromous changes of α-SMA and Collagen I protein levels with P-Smad2/3L in each group were emerged in cultured HSCs (HSCs named HSC-T6 cells employed) (Fig. 6). These results suggest that Sal B exerts anti-liver fibrosis effects involved in MAPK-mediated Smad2/3 linker regions phosphorylation.

3.7. MAPK inhibitors heightened inhibiting effects of Sal B on TGF-β_1-induced activation and Collagen I production of HSCs involved in inhibition of Smad2/3 linker regions phosphorylation

In view of the phosphorylation of Smad2/3 at linker regions depended on activation of MAPKs, inhibited activation of MAPKs and phosphorylation of Smad2/3 linker regions were observed in TGF-β_1-activated HSCs by Sal B treatment, therefore it was speculated that MAPK-mediated Smad2/3 phosphorylation at linker regions might be pivotal link of Sal B-mediated TGF-β signaling. We investigated the effects of Sal B on HSCs activation and Collagen I production involved in Smad2/3 linker regions phosphorylation under inhibited activation of MAPKs using MAPK inhibitors. Results showed that down-regulated protein levels of P-MAPKs (Including P-ERK1/2, P-JNK1/2 and P-p38 respectively) in MAPK inhibitors (Including PD98059, SP600125 and SB203580 respectively) treatment-group were presented, and co-

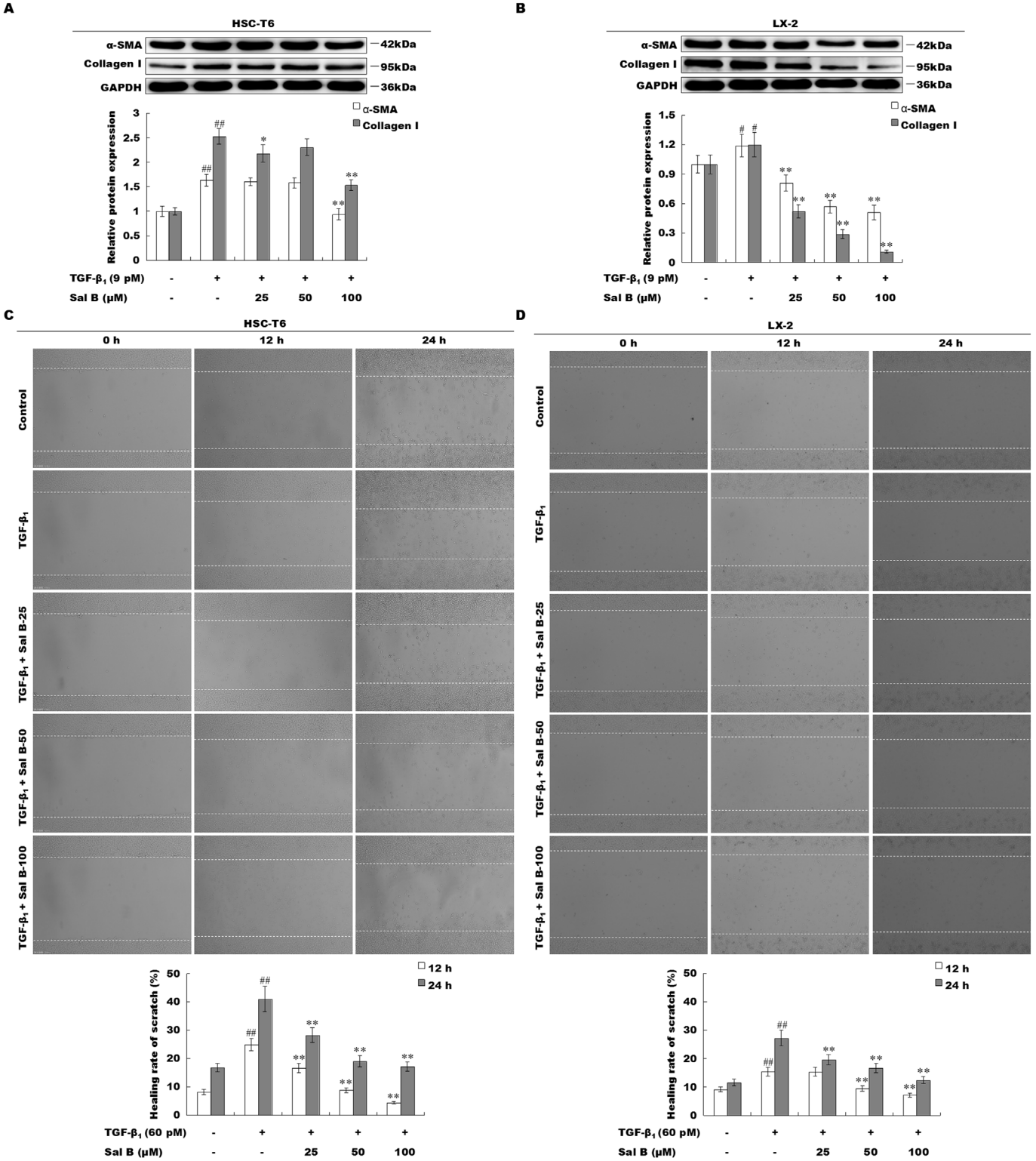

Fig. 2. Sal B repressed hepatic-fibrosis markers expression and cell migration in TGF-β_1-activated HSCs. (A) and (B) HSCs including rat HSC-T6 and human LX-2 cells were treated with or without Sal B (25 μM, 50 μM, 100 μM) for 24 h and TGF-β_1 (9 pM) for 1 h, total proteins were extracted and hepatic-fibrosis markers including α-SMA and Collagen I were measured by Western blot. Representative images in each group were presented, semiquantitative analyses of α-SMA and Collagen I were respectively conducted, GAPDH was deemed as the loading control, the ratio of α-SMA or Collagen I protein to GAPDH in control group was assigned a value of 1. Data were expressed as mean ± SD, n = 3 (Based on three independent experiments). $^{\#}P < 0.05$, $^{\#\#}P < 0.01$ versus control group; $^{*}P < 0.05$, $^{**}P < 0.01$ versus TGF-β_1 alone stimulated group. (C) and (D) HSCs including HSC-T6 and LX-2 cells were treated with or without Sal B (25 μM, 50 μM, 100 μM) and TGF-β_1 (60 pM) for 24 h. Cell migration was assessed by Scratch test and image acquisition with scratch area performed at 0, 12, 24 h window respectively, representative images in each group were presented. Quantitative analyses of cell migration were calculated according to the following formula: Healing rate of scratch (%) = (the width of scratch area at 0 h - the width of scratch area at 12/24 h) ÷ the width of scratch area at 0 h × 100%. Data were expressed as mean ± SD, n = 3 (Based on three independent experiments). $^{\#\#}P < 0.01$ versus control group; $^{**}P < 0.01$ versus TGF-β_1 alone stimulated group.

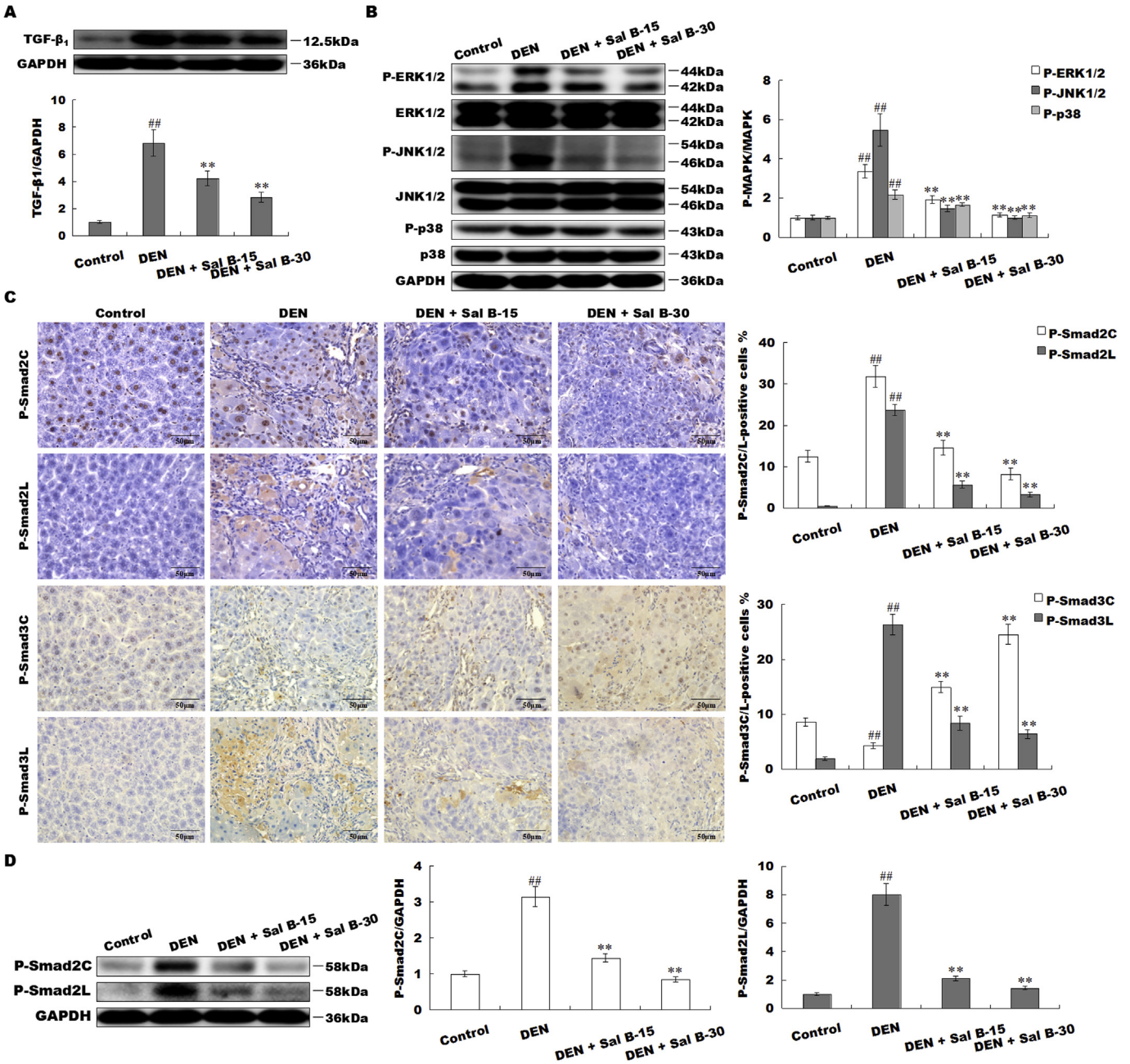

Fig. 3. Sal B inhibited the activation of MAPK pathways and modulated the phosphorylation of Smad2/3 in mice with DEN-induced liver fibrosis. (A) and (B) Protein levels of TGF-β_1 and activated MAPKs including phosphorylated (P)-ERK1/2, P-JNK1/2, P-p38 from mouse liver tissues were measured by Western blot and representative images in each group were presented. Semiquantitative analyses of above proteins were respectively conducted, GAPDH and/or MAPKs including ERK1/2, JNK1/2 and p38 were deemed as the loading control respectively and the ratio of each measured protein to corresponding loading control in control group was assigned a value of 1. Data were expressed as mean ± SD, n = 3. $^{\#\#}P < 0.01$ versus control group; $^{**}P < 0.01$ versus DEN group. (C) Protein expressions of phosphorylated Smad2/3 at terminal (P-Smad2C/P-Smad3C) and linker regions (P-Smad2L/P-Smad3L) were detected by Immunohistochemical staining and representative images in each group were presented (Magnification × 400). Quantification of P-Smad2C-, P-Smad2L-, P-Smad3C- and P-Smad3L-positive cells (Brown color) were respectively conducted, data were expressed as mean ± SD, n = 8. $^{\#\#}P < 0.01$ versus control group; $^{**}P < 0.01$ versus DEN group. (D) Protein expressions of P-Smad2C and P-Smad2L were measured by Western blot and representative images in each group were presented. Semiquantitative analyses of P-Smad2C and P-Smad2L protein levels were respectively conducted, GAPDH was deemed as the loading control and the ratio of P-Smad2C or P-pSmad2L protein to GAPDH in control group was assigned a value of 1. Data were expressed as mean ± SD, n = 3. $^{\#\#}P < 0.01$ versus Control group; $^{**}P < 0.01$ versus DEN group. (For interpretation of the references to color in this figure legend, the reader is referred to the Web version of this article.)

treatment of Sal B (50 μM) led to lower protein levels of P-MAPKs compared to those of MAPK inhibitors treatment-group in cultured HSCs (HSCs named HSC-T6 cells employed); synchronously, co-down-regulated protein levels of α-SMA and Collagen I were observed in MAPK inhibitors treatment-group, and more reduced in co-treatment of Sal B (50 μM), homodromous changes of protein levels between P-Smad2/3L and α-SMA/Collagen I were present in the absence or presence of MAPK inhibitors and/or Sal B treatment (Fig. 7). These results indicate that MAPK inhibitors heightens inhibiting effects of Sal B on TGF-β_1-induced activation and Collagen I production of HSCs involved in inhibition of Smad2/3 linker regions phosphorylation.

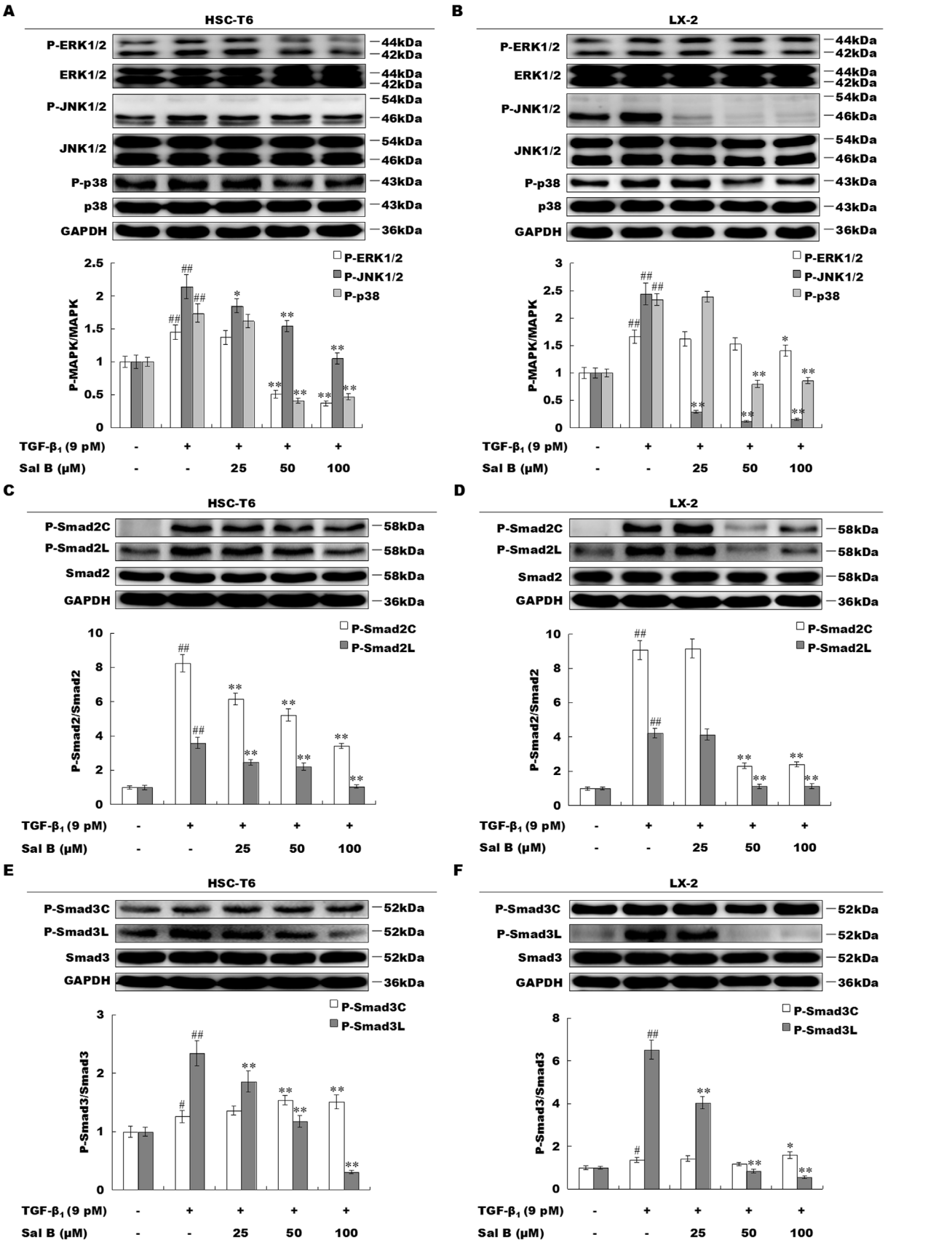

(caption on next page)

Fig. 4. Sal B modulated MAPK pathways activation and Smad2/3 phosphorylation in TGF-β_1-activated HSCs. (A–D) HSCs including rat HSC-T6 and human LX-2 cells were treated with or without Sal B (25 μM, 50 μM, 100 μM) for 24 h and TGF-β_1 (9 pM) for 1 h, total proteins were extracted and phosphorylated (P)-ERK1/2, P-JNK1/2, P-p38, P-Smad2C, P-Smad2L, P-Smmad3C and P-Smad3L were measured by Western blot, representative images in each group were presented. Semiquantitative analyses of above proteins were respectively conducted, MAPKs including ERK1/2, JNK1/2 and p38, Smad2, Smad3 and GAPDH were deemed as the loading control respectively, the ratio of each measured protein to corresponding loading control in control group was assigned a value of 1. Data were expressed as mean ± SD, n = 3 (Based on three independent experiments). $^{\#}P < 0.05$, $^{\#\#}P < 0.01$ versus control group; $^{*}P < 0.05$, $^{**}P < 0.01$ versus TGF-β_1 alone stimulated group.

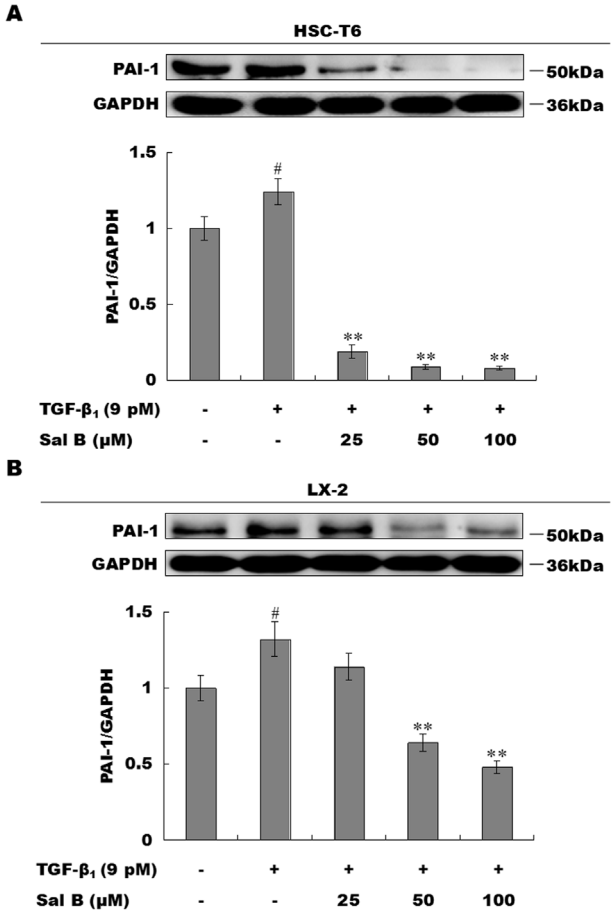

Fig. 5. Sal B down-regulated PAI-1 protein expression in TGF-β_1 activated HSCs. (A) and (B) HSCs including rat HSC-T6 and human LX-2 cells were treated with or without Sal B (25 μM, 50 μM, 100 μM) for 24 h and TGF-β_1 (9 pM) for 1 h, total proteins were extracted and protein level of PAI-1 was measured by Western blot, representative image in each group was presented. Semiquantitative analysis of PAI-1 was conducted, GAPDH was deemed as the loading control, the ratio of PAI-1 protein to GAPDH in control group was assigned a value of 1. Data were expressed as mean ± SD, n = 3 (Based on three independent experiments). $^{\#}P < 0.05$ versus control group; $^{**}P < 0.01$ versus TGF-β_1 alone stimulated group.

4. Discussion

Here, we stated a novel molecular mechanism of Sal B as a potential anti-liver fibrosis drug *via* regulating MAPK-mediated Smad2/3 phosphoisoform signaling *in vivo* and *in vitro*. These results from the study showed Sal B observably inhibited the activation of MAPKs and then decreased P-Smad2L/P-Smad3L protein levels, ultimately down-regulated the expression of its downstream fibrogenic gene PAI-1, which might be a crucial molecular mechanism of Sal B's anti-liver fibrosis effects. The detailed discussion was as follows.

Sal B, a main family member of water-soluble phenolic acids regarded as the predominant active ingredients of *Salvia miltiorrhiza* Bunge, possesses multiple bio-activities such as anti-oxidative, anti-inflammatory, anti-viral, anti-fibrotic and anti-tumour activities [23]. Here, our research focused on Sal B's anti-fibrotic effects on hepato-fibrogenesis and progression, which displayed excellent activity of Sal B against liver fibrosis reflected in ameliorative histopathological characteristics and lower levels of hepatic-fibrosis markers including α-SMA and Collagen I in *in vivo* model of liver fibrosis induced by DEN in mice (Fig. 1), subdued cell migration capacity and reduced Collagen I production in TGF-β_1 activated HSCs including rat HSC-T6 and human LX-2 cell lines *in vitro* models of liver fibrosis (Fig. 2). These results are matched with previous reports that Sal B protects against CCl_4-and/or DMN-induced liver fibrosis in rats or mice and inhibits activation and collagen production in cultured primary rat-HSCs [15,16,20,24], and enrich the evidences for Sal B's anti-hepatic fibrosis activity.

Undoubtedly, the pathomechanism of hepato-fibrogenesis-progress is very complicated, which is implicated in polytype cells and multiple signaling pathways/molecules [25]. Among those, the persistent activation and succedent phenotype transformation of HSCs to myofibroblasts induced by pro-fibrogenic cytokines are dominant events leading to hepato-fibrogenesis [3]. TGF-β_1 is a well-proven powerfully pro-fibrogenic cytokine especially directing at liver fibrosis [26]. Although a few reports have shown that Sal B exerts anti-liver fibrosis effects involved in TGF-β signaling, for instance, Sal B can decrease protein levels of TGF-β_1 and TβRI in rat's fibrotic liver induced by DMN and down-regulate the kinase activity of TβRI and protein levels of Smad2/3 in primary rat-HSCs activated by TGF-β_1 [16,17,27], Sal B can inhibit the activation of ERK and p38 MAPK pathways in TGF-β_1-stimulated primary rat-HSCs [28]. However, the exactly adjusted mechanism of Sal B on TGF-β signaling, especially Smad2/3 phosphoisoform signaling remains inconclusive. Since Smad2/3, two crucial intracellular mediators downstream of TGF-β signaling, play a direct role of signal extraction *via* selectively activating Smad2/3 at C-terminal and/or linker regions depended on TβRI and MAPK respectively [29]. Activated MAPKs phosphorylate Smad2/3 at linker regions to contribute fibrogenic effects of TGF-β signaling *via* accelerating collagen production and enhancing athletic ability in human mesangial cells and rat liver myofibroblasts [30–32]. Earlier, our studies also found that inhibited activation of MAPKs using MAPK inhibitors including ERK-specific inhibitor (PD98059), JNK-specific inhibitor (SP600125) and p38-specific inhibitor (SB203580) mediated TGF-β_1/Smad signaling *via* suppressing Smad2/3 linker regions phosphorylated in keloid fibroblasts and liver myofibroblasts rooted from primary rat-HSCs [33,34]. Therefore, our study centered on addressing Sal B's mediated mechanism involved in Smad2/3 phosphoisoform signaling, especially MAPK-mediated Smad2/3 linker regions phosphorylation in liver fibrosis. Firstly, Sal B's mediated effects on the protein expression of TGF-β_1/MAPK/Smad2/3 signaling axis were assessed and compared in *in vivo* model of liver fibrosis induced by DEN in Kunming mice, which showed that significantly increased protein expressions of TGF-β_1 and P-MAPKs (Including P-ERK1/2, P-JNK1/2 and P-p38) were observed in liver tissues of mice only administrated by DEN for 12 weeks, while markedly decreased by incorporative treatment using Sal B with two doses of 15 and 30 mg/kg (Fig. 3A and B), which were consistent with earlier findings that Sal B inhibited TGF-β_1 over-expression and MAPK activation in *in vivo* model of liver fibrosis induced by CCl_4 and/or DMN in rats [16,28]. Phosphorylated Smad2/3 at terminal and linker regions (P-Smad2C/L and P-Smad3C/L) create 3 types of major intracellular signaling below: ① cytostatic P-Smad3C signaling, ② mitogenic P-Smad3L signaling, ③ invasive/migratory/fibrogenic P-Smad2L/C or P-Smad3L signaling [7].

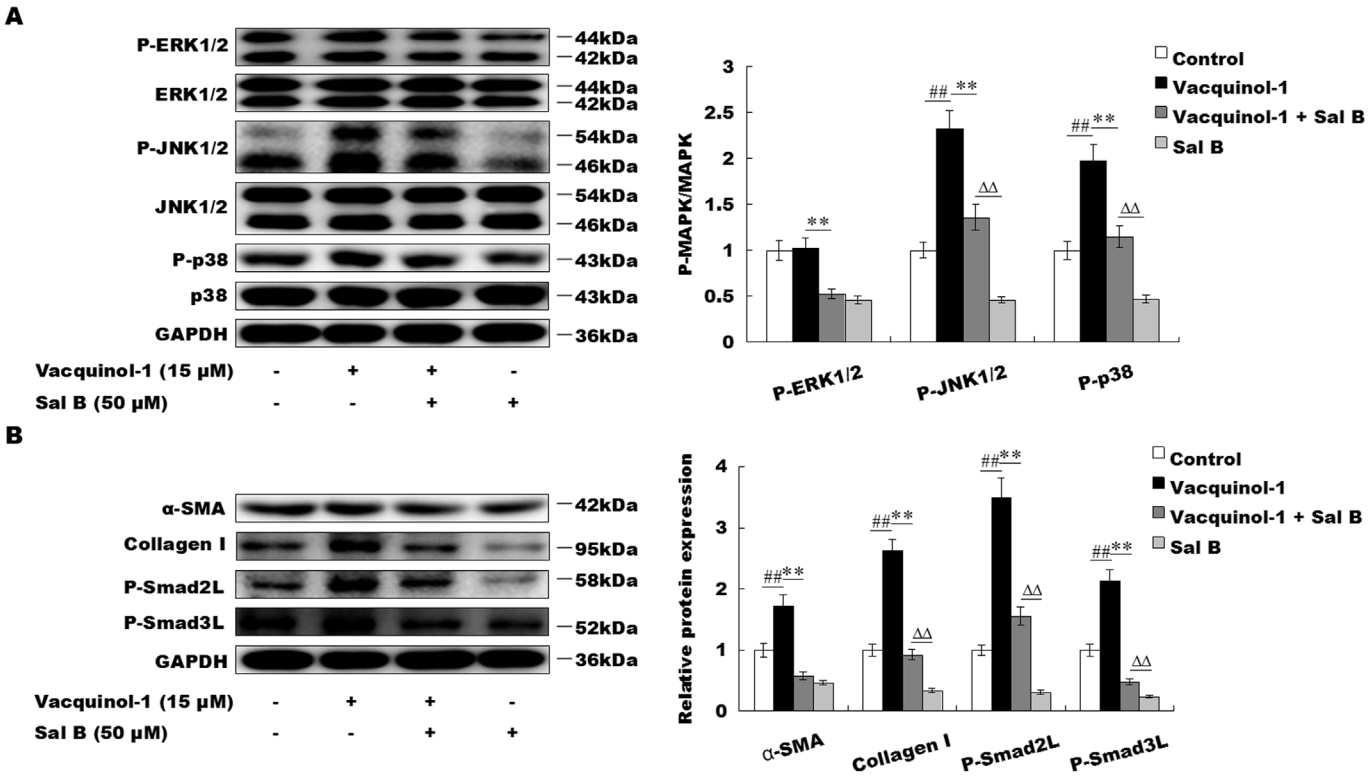

Fig. 6. MAPK activator receded inhibitory effects of Sal B on HSCs activation and Collagen I production involved in enhancement of Smad2/3 linker regions phosphorylation. (A–B) HSCs named HSC-T6 cells were treated with or without Sal B (50 μM) for 24 h and MAPK activator (Vacquinol-1, 15 μM) for 5 h, total proeins were extracted and protein levels of P-ERK1/2, P-JNK1/2, P-p38, α-SMA, Collagen I, P-Smad2L and P-Smad3L were measured by Western blot and representative images in each group were presented. Semiquantitative analyses of above proteins were respectively conducted, ERK1/2, JNK1/2, p38 and GAPDH were deemed as the loading control respectively, the ratio of each measured protein to corresponding loading control in control group was assigned a value of 1. Data were expressed as mean ± SD, n = 3 (Based on three independent experiments). $^{\#\#}P < 0.01$, $^{**}P < 0.01$, $^{\Delta\Delta}P < 0.01$.

Coincidentally, our results showed that DEN induced increased both P-Smad2L/C- and P-Smad3L-positive cells while decreased P-Smad3C-positive cells in liver tissues, particularly conspicuous increase of P-Smad2L- and P-Smad3L-positive cells in these areas with fibrotic lesions, however, above observations were reversely changed with accompanied Sal B treatment (Fig. 3C); significantly increased protein levels of P-Smad2L/C were observed in liver tissues from DEN group while decreased P-Smad2L/C by Sal B treatment were presented using Western blot analysis (Fig. 3D), and previous finding that Sal B increased protein level of P-Smad3C while decreased P-Smad3L in liver tissues with fibrosis induced by DEN in mice by Western blot analysis [35], which were complementary and consistent with above results by Immunohistochemical staining analysis. These results *in vivo* imply Sal B's anti-liver fibrosis effects associated with mediated TGF-β/MAPK/Smad signaling pathway, especially inhibited MAPK-dependent P-Smad2/3 at linker regions. Secondly, *In vitro* experiments were conducted to proof above implication using cell model of liver fibrosis, which showed that Sal B markedly decreased protein expressions of P-ERK1/2, P-JNK1/2, P-p38, P-Smad2C, P-Smad2L and P-Smad3L elevated by TGF-β_1 in both rat-HSCs (HSC-T6) and human-HSCs (LX-2), together with down-regulated protein level of PAI-1, a critical target gene of TGF-β signaling contributing to hepato-fibrogenesis and progression; synchronously, Sal B slightly increased protein expressions of P-Smad3C (Figs. 4 and 5). These results highlight that MAPK-mediated TGF-β signaling *via* phosphorylating Smad2/3 at linker regions could be important pharmacological targets of Sal B's against liver fibrosis effects.

Further, we verified above speculation using MAPK activator/inhibitor to up-regulate and/or down-regulate P-MAPK protein levels, then observed Sal B's anti-fibrosis effects involved in MAPK-mediated Smad2/3 phosphorylation at linker regions using HSCs (HSC-T6 cell line). Our results showed that observably increased protein expressions of Smad2/3 at linker regions (P-Smad2L/P-Smad3L) when MAPKs were activated by MKK4-specific activator (Vacquinol-1) or TGF-β_1, together with increased α-SMA and Collagen I protein expressions, while combined Sal B treatment antagonized above effects; moreover, inhibited activation of MAPKs using MAPK inhibitors (PD98059: ERK-specific inhibitor; SP600125: JNK-specific inhibitor; SB203580: p38-specific inhibitor) produced synergistically inhibited effects on P-Smad2L, P-Smad3L, α-SMA and Collagen I protein expressions with Sal B (Figs. 6 and 7). Above observed results are in coincident with the accepted theory that MAPK-mediated Smad2/3 linker regions phosphorylation contributing to hepato-fibrogenesis and progression, which suggest that Sal B exerts against liver fibrosis effects associated with inhibiting MAPK-mediated Smad2/3 linker regions phosphorylation.

Taken together, these presented results enrich the evidences for Sal B against liver fibrosis effects and state Sal B's mechanism of action involved in Smad2/3 phosphoisoform signaling, especially inhibited MAPK-mediated phospho-Smad2/3 at linker regions. However, some further questions have been also raised, for example, whether Sal B would possess anti-inflammatory properties in other nonparenchymal and parenchymal liver cells involved in mediation of TGF-β signaling, which is the actual target of Sal B, and so on. Therefore, further studies need be conducted in a near future.

5. Conclusions

Sal B alleviates DEN-caused liver fibrosis embodied in decreased protein levels of hepatic markers (α-SMA, Collagen I, TGF-β_1) and ameliorative histopathological characteristics in *in vivo* model, and impedes TGF-β_1-driven cell migration and Collagen I production of HSCs *in vitro* model. The underlying molecular mechanism associated

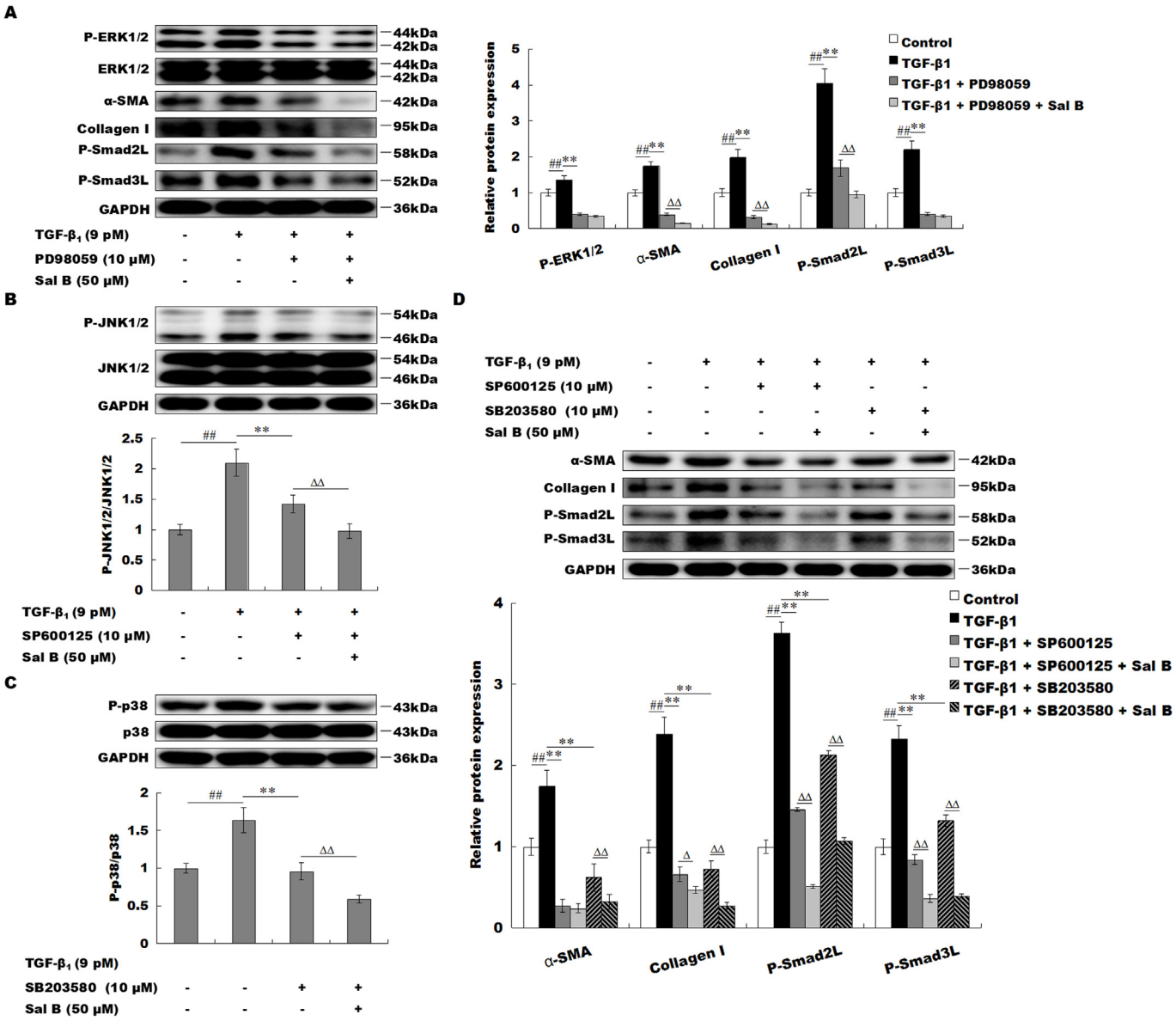

Fig. 7. MAPK inhibitors heightened inhibitory effects of Sal B on TGF-β_1-induced activation and Collagen I production of HSCs involved in inhibition of Smad2/3 linker regions phosphorylation. (A–D) HSCs named HSC-T6 cells were treated with or without Sal B (50 μM) for 24 h and three MAPK inhibitors (PD98059, 10 μM; SP600125, 10 μM; SB203580, 10 μM) for 5 h, and TGF-β_1 (9 pM) for 1 h, total proteins were extracted and protein levels of P-ERK1/2, P-JNK1/2, P-p38, α-SMA, Collagen I, P-Smad2L and P-Smad3L were measured by Western blot and representative images in each group were presented. Semiquantitative analyses of above proteins were respectively conducted, ERK1/2, JNK1/2, p38 and GAPDH deemed as the loading control respectively, the ratio of each measured protein to corresponding loading control in control group was assigned a value of 1. Data were expressed as mean ± SD, n = 3 (Based on three independent experiments). $^{\#\#}P < 0.01$, $^{*}P < 0.05$, $^{**}P < 0.01$, $^{\Delta}P < 0.05$, $^{\Delta\Delta}P < 0.01$.

with TGF-β/Smad signaling and MAPK pathways, especially inhibited MAPK-mediated P-Smad2/3 at linker regions. These results highlight MAPK-mediated P-Smad2/3L as a pivotal target for antifibrotic therapy and Sal B as a potential anti-liver fibrosis drug *via* inhibiting MAPK-mediated P-Smad2/3L signaling.

Author's contribution

Yan Yang conceived, designed and supervised the research project, received funding; Chao Wu, Weiyang Chen, Hanyan Ding, Dong Li, Guanghua Wen, Chong Zhang, Wanpeng Lu and Ming Chen performed the research project; Chao Wu analyzed experimental data, interpreted experimental results and drafted the manuscript; Yan Yang reviewed the manuscript.

Declaration of competing interest

The authors declare that there are no conflicts of interest.

Acknowledgements

This work was financially supported from the National Natural Science Foundation of China (No. 81573652, 81874354 and 81801064). Also, we are grateful that Prof. Koichi Matsuzaki (Department of Gastroenterology and Hepatology, Kansai Medical University, Osaka, Japan) provides the specific antibodies (Rabbit anti-P-Smad2L antibody; rabbit anti-P-Smad3L antibody) for us.

References

[1] P. Kocabayoglu, S.L. Friedman, Cellular basis of hepatic fibrosis and its role in inflammation and cancer, Front. Biosci. 5 (2013) 217–230.
[2] Y.A. Lee, M.C. Wallace, S.L. Friedman, Pathobiology of liver fibrosis: a translational success story, Gut 64 (5) (2015) 830–841.
[3] T. Kisseleva, D.A. Brenner, Role of hepatic stellate cells in fibrogenesis and the reversal of fibrosis, J. Gastroenterol. Hepatol. 22 (Suppl 1) (2007) S73–S78.
[4] D. Javelaud, A. Mauviel, Mammalian transforming growth factor-betas: Smad signaling and physio-pathological roles, Int. J. Biochem. Cell Biol. 36 (7) (2004) 1161–1165.
[5] L. Yang, S. Inokuchi, Y.S. Roh, J. Song, R. Loomba, E.J. Park, E. Seki, Transforming growth factor-beta signaling in hepatocytes promotes hepatic fibrosis and carcinogenesis in mice with hepatocyte-specific deletion of TAK1, Gastroenterology 144 (5) (2013) 1042–1054 e4.
[6] K. Yoshida, M. Murata, T. Yamaguchi, K. Matsuzaki, TGF-beta/Smad signaling during hepatic fibro-carcinogenesis (review), Int. J. Oncol. 45 (4) (2014) 1363–1371.
[7] K. Matsuzaki, Smad phospho-isoforms direct context-dependent TGF-beta signaling, Cytokine Growth Factor Rev. 24 (4) (2013) 385–399.
[8] P. Flevaris, D. Vaughan, The role of plasminogen activator inhibitor type-1 in fibrosis, Semin. Thromb. Hemost. 43 (2) (2017) 169–177.
[9] K. Matsuzaki, Modulation of TGF-beta signaling during progression of chronic liver diseases, Front. Biosci. (Landmark Ed) 14 (2009) 2923–2934.
[10] J.J. Zheng, P.H. Dong, Y.Q. Mao, S.L. Chen, X.L. Wu, G.J. Li, Z.Q. Lu, F.J. Yu, lincRNA-p21 inhibits hepatic stellate cell activation and liver fibrogenesis via p21, FEBS J. 282 (24) (2015) 4810–4821.
[11] G.H. Du, J.T. Zhang, Research progress of water-soluble active ingredients of Salvia miltiorrhiza Bunge - salvianolic acids, Basic Med. Sci. Clin. 20 (5) (2000) 394–398.
[12] W. Chen, G.X. Chen, Danshen (Salvia miltiorrhiza Bunge): a prospective healing sage for cardiovascular diseases, Curr. Pharmaceut. Des. 23 (34) (2017) 5125–5135.
[13] S. Li, N. Wang, M. Hong, H.Y. Tan, G.F. Pan, Y.B. Feng, Hepatoprotective effects of a functional formula of three Chinese medicinal herbs: experimental evidence and network pharmacology-based identification of mechanism of action and potential bioactive components, Molecules 23 (2) (2018) E352 pii.
[14] P. Liu, Y.Y. Hu, C. Liu, D.Y. Zhu, H.M. Xue, Z.Q. Xu, L.M. Xu, C.H. Liu, H.T. Gu, Z.Q. Zhang, Clinical observation of salvianolic acid B in treatment of liver fibrosis in chronic hepatitis B, World J. Gastroenterol. 8 (4) (2002) 679–685.
[15] H.Y. Gao, G.Y. Li, M.M. Lou, X.Y. Li, X.Y. Wei, J.H. Wang, Hepatoprotective effect of matrine salvianolic acid B salt on carbon tetrachloride-induced hepatic fibrosis, J. Inflamm. 9 (1) (2012) 16.
[16] Y.Y. Tao, Q.L. Wang, L. Shen, W.W. Fu, C.H. Liu, Salvianolic acid B inhibits hepatic stellate cell activation through transforming growth factor beta-1 signal transduction pathway in vivo and in vitro, Exp. Biol. Med. 238 (11) (2013) 1284–1296.
[17] C. Liu, P. Liu, Y.Y. Hu, D.Y. Zhu, Effects of salvianolic acid-B on TGF-beta 1 stimulated hepatic stellate cell activation and its intracellular signaling, Zhonghua Yixue Zazhi 82 (18) (2002) 1267–1272.
[18] Y. Kan, Y. Yang, Effect of salvianolic acid B on apoptosis of liver fibrotic cells based on cleaved caspase-9 protein, Chin. Pharmacol. Bull. 45 (6) (2019) 827–832.
[19] H.J. Yang, G.L. Liu, B. Liu, T. Liu, GP73 promotes invasion and metastasis of bladder cancer by regulating the epithelial-mesenchymal transition through the TGF-beta1/Smad2 signalling pathway, J. Cell Mol. Med. 22 (3) (2018) 1650–1665.
[20] R. Wang, X.Y. Yu, Z.Y. Guo, Y.J. Wang, Y. Wu, Y.F. Yuan, Inhibitory effects of salvianolic acid B on CCl(4)-induced hepatic fibrosis through regulating NF-kappaB/IkappaBalpha signaling, J. Ethnopharmacol. 144 (3) (2012) 592–598.
[21] J.J. Wang, J. Li, L. Shi, X.W. Lv, W.M. Chen, Y.Y. Chen, Preventive effects of a fractioned polysaccharide from a traditional Chinese herbal medical formula (Yu Ping Feng San) on carbon tetrachloride-induced hepatic fibrosis, J. Pharm. Pharmacol. 62 (7) (2010) 935–942.
[22] A. Boye, C. Wu, Y.F. Jiang, J.Y. Wang, J.J. Wu, X.C. Yang, Y. Yang, Compound Astragalus and Salvia miltiorrhiza extracts modulate MAPK-regulated TGF-β/Smad signaling in hepatocellular carcinoma by multi-target mechanism, J. Ethnopharmacol. 169 (2015) 219–228.
[23] M. Shi, F.F. Huang, C.P. Deng, Y. Wang, G.Y. Kai, Bioactivities, biosynthesis and biotechnological production of phenolic acids in Salvia miltiorrhiza, Crit. Rev. Food Sci. Nutr. 59 (6) (2019) 953–964.
[24] Y.L. Lin, C.H. Wu, M.H. Luo, Y.J. Huang, C.N. Wang, M.S. Shiao, Y.T. Huang, In vitro protective effects of salvianolic acid B on primary hepatocytes and hepatic stellate cells, J. Ethnopharmacol. 105 (1–2) (2006) 215–222.
[25] G.O. Elpek, Cellular and molecular mechanisms in the pathogenesis of liver fibrosis: an update, World J. Gastroenterol. 20 (23) (2014) 7260–7276.
[26] S. Dooley, P. ten Dijke, TGF-β in progression of liver disease, Cell Tissue Res. 347 (1) (2012) 245–256.
[27] J.F. Zhao, C.H. Liu, Y.Y. Hu, L.M. Xu, P. Liu, C. Liu, Effect of salvianolic acid B on Smad3 expression in hepatic stellate cells, Hepatobiliary Pancreat. Dis. Int. 3 (1) (2004) 102–105.
[28] Z.G. Lv, Y.F. Song, D.Y. Xue, W.W. Zhang, Y. Cheng, L.M. Xu, Effect of salvianolic-acid B on inhibiting MAPK signaling induced by transforming growth factor-beta1 in activated rat hepatic stellate cells, J. Ethnopharmacol. 132 (2) (2010) 384–392.
[29] K. Matsuzaki, Smad phosphoisoform signaling specificity: the right place at the right time, Carcinogenesis 32 (11) (2011) 1578–1588.
[30] F. Furukawa, K. Matsuzaki, S. Mori, Y. Tahashi, K. Yoshida, Y. Sugano, H. Yamagata, M. Matsushita, T. Seki, Y. Inagaki, M. Nishizawa, J. Fujisawa, K. Inoue, p38 MAPK mediates fibrogenic signal through Smad3 phosphorylation in rat myofibroblasts, Hepatology 38 (4) (2003) 879–889.
[31] T. Hayashida, M. Decaestecker, H.W. Schnaper, Cross-talk between ERK MAP kinase and Smad signaling pathways enhances TGF-beta-dependent responses in human mesangial cells, FASEB J. 17 (11) (2003) 1576–1578.
[32] K. Yoshida, K. Matsuzaki, S. Mori, Y. Tahashi, H. Yamagata, F. Furukawa, T. Seki, M. Nishizawa, J. Fujisawa, K. Okazaki, Transforming growth factor-beta and platelet-derived growth factor signal via c-Jun N-terminal kinase-dependent Smad2/3 phosphorylation in rat hepatic stellate cells after acute liver injury, Am. J. Pathol. 166 (4) (2005) 1029–1039.
[33] S.F. He, X. Liu, Y. Yang, W.J. Huang, S.X. Xu, S. Yang, X.J. Zhang, Mechanisms of transforming growth factor b1/Smad signalling mediated by mitogen-activated protein kinase pathways in keloid fibroblasts, Br. J. Dermatol. 162 (3) (2010) 538–546.
[34] Y.F. Jiang, C. Wu, A. Boye, J.J. Wu, J.Y. Wang, X.C. Yang, Y. Yang, MAPK inhibitors modulate Smad2/3/4 complex cyto-nuclear translocation in myofibroblasts via Imp7/8 mediation, Mol. Cell. Biochem. 406 (1–2) (2015) 255–262.
[35] Y. Ma, M. Fang, C. Wu, Y.Y. Xu, X.M. Tao, T.J. Wang, Z. Nuo, B.G. Du, Y. Yang, Salvianolic acid B exerts anti-hepatic fibrosis-carcinoma effect via mediation of pSmad3C/pSmad3L, Chin. Pharmacol. Bull. 34 (1) (2018) 44–50.